

Possible 4d ferromagnetism of Rh and Ru overlayers on a Ag(001) substrate

Ruqian Wu

Department of Physics and Astronomy, Northwestern University, Evanston, Illinois 60208-3112

A. J. Freeman

*Department of Physics and Astronomy, Northwestern University, Evanston, Illinois 60208-3112
and Materials Science Division, Argonne National Laboratory, Argonne, Illinois 60439*

(Received 17 October 1991)

The possibility of 4d ferromagnetism is explored for Rh and Ru overlayers on a Ag(001) substrate using the full-potential linearized augmented-plane-wave method. The overlayer relaxation is found to be very small and to have no significant effect on the electronic and magnetic properties. The ferromagnetism of Rh/Ag(001) can be destroyed by an additional Ag layer—which attributes the lack of ferromagnetism in recent surface magneto-optic Kerr-effect experiments to the surface segregation between Rh and Ag atoms. However, Ru/Ag(001) is predicted to be ferromagnetic with both a larger magnetic moment and larger magnetic energy even after being covered by a Ag layer, and thus is more suitable for experimental verification. For both the Rh and Ru cases, the total hyperfine field is predicted to be too small for detecting these possible magnetism. Finally, the considerably strong overlayer-substrate Coulomb repulsion effect indicates that Ag is no longer the “benign” substrate for 4d overlayer magnetism that it is for the 3d metals.

I. INTRODUCTION

Fortunately today, it is possible to synthesize and study high-quality ultrathin metal films on various substrates. This has dramatically and importantly increased the number and variety of magnetic materials and has challenged theory for understanding magnetism in low-dimensional systems.^{1,2} It is well recognized now that environments with fewer nearest neighbors and hence weaker interatomic hybridization are conducive to enhanced magnetization.^{3,4} Naturally, questions have been raised, because of its inherent interest and importance to both fundamental studies and practical applications, whether nonmagnetic (PM) metals in the bulk (e.g., the 4d metals) may become ferromagnetic (FM) at the surface or in an epitaxial overlayer. This possibility can be expected because some 4d metals (e.g., Pd) are known to exhibit incipient magnetic behavior and large paramagnetic susceptibilities.

In a pioneering work, Brodsky and Freeman⁵ synthesized and studied the magnetic properties of Pd sandwiched by Au. The expectation was that the expansion of the Pd lattice constant by the larger Au lattice constant would narrow its 4d band and subsequently increase the Stoner factor and thus drive the system to ferromagnetism. In this experiment,⁵ they found an exceptionally large increase in the magnetic susceptibility of thin films of Pd sandwiched by Au films at low temperature. In a later experiment,⁶ a small magnetic moment was found. Theoretically, Jarlborg and Freeman⁷ reported a greatly enhanced susceptibility for the Au/Pd/Au sandwich using the linear muffin-tin orbital (LMTO) method. Recent full-potential linearized augmented-plane-wave (FLAPW) calculations carried out by Hong,

Fu, and Freeman⁸ indeed confirmed the ferromagnetism in a Au/Pd/Au sandwich with a magnetic moment that was small ($0.02 \mu_B$) and close to the experimental value.⁶ Moruzzi and Marcus and Chen, Brener, and Callaway also found that susceptibility of Pd and other 4d metals increases with volume and may lead to a PM-FM [or antiferromagnetic (AFM)] phase transition in the bulk.

More recently, according to the calculated results by Zhu, Bylander, and Kleinman,¹¹ a Pd monolayer is FM (with a magnetic moment of $0.4 \mu_B/\text{atom}$) over a wide range of interatomic spacings. Ru and Rh monolayers were also found to form an even stronger FM state.^{4,12} However, to verify these theoretical predictions of 4d ferromagnetism in lower dimensions, ultrathin 4d metal films must be grown epitaxially on a substrate. Of course, the additional substrate may affect the overlayer magnetism significantly even though the overlayer-substrate interaction may be “very weak.” For example, an isolated V(001) monolayer is ferromagnetically ordered, but the coupling changes dramatically to AFM ordering when deposited on a Ag(001) substrate.¹³ A strong decrease of the magnetic moment was also found for Ni/Cu(111) (Ref. 14) and the Ag/Ni/Ag(001) sandwich was reported to be even magnetically dead¹⁵ although the Cu and Ag substrates are known to be magnetically inert in many systems.⁴ Furthermore, since the 4d wave function is more spatially extended compared to the 3d's, their magnetic properties are expected to be more sensitive to any small change of the environment. Indeed, the Pd monolayer was found to lose its magnetism on the Ag(001) surface^{11,16} and, as stated, the magnetic moment decreases to only $0.02 \mu_B$ in a Au/Pd/Au sandwich.⁸ Pd(001) and Pd(111) (Refs. 4 and 17) are predicted to be magnetically dead despite the expectation of magnetic moment

enhancement at the surface. Therefore, the substrate effect has to be included when 4d ferromagnetism is discussed.

Strikingly, Zhu, Bylander, and Kleinman¹⁸ (using norm-conserving pseudopotentials with a Gaussian-orbital expansion) and Eriksson, Albers, and Boring¹⁹ [using a linear muffin-tin orbital (LMTO) film code with the fixed spin-moment method²⁰] obtained large ferromagnetic moments ($1.09\mu_B$ and $0.62\mu_B$, respectively) for Rh/Ag(001) and Rh/Au(001). Eriksson, Albers, and Boring also showed that FM ordering may also exist in Ru/Ag(001) but only as a metastable state.¹⁹ By contrast, recent verification experiments using the surface magneto-optic Kerr effect²¹ (SMOKE) failed to find any evidence of ferromagnetism in Rh/Ag(001) at temperatures down to 40 K.^{22,23} Three possibilities were proposed to explain the discrepancy²²: (1) surface segregation between Rh and Ag atoms, which may result in the covering of the Rh film by a Ag monolayer; (2) interdiffusion caused by intermixing with the Ag matrix resulting in a dilution of the Rh below the percolation threshold; (3) the reliability of the theoretical calculations. The first factor may be tested theoretically. The second factor is unlikely because, as reported by Mulhollan, Fink, and Erskine,²² the deposition of $\sim 15\%$ more Rh does not change the SMOKE signal. The third factor should be checked carefully since possible overlayer relaxation was not included in both calculations^{18,19} and, furthermore, the accuracy of pseudopotential and LMTO schemes may also be questionable for transition-metal surfaces or interfaces. For example, the calculated magnetic moments differ by as much as a factor of 2 in these two studies ($0.62\mu_B$ by Eriksson, Albers, and Boring¹⁹ and $1.09\mu_B$ by Zhu, Bylander, and Kleinman¹⁸). Finally, Zhu, Bylander, and Kleinman did not compare the cohesive energies of the PM and FM states¹⁸ so that it is not known which is the lower-energy state.

In this work, the results of highly precise FLAPW calculations carried out to determine the possibility of 4d ferromagnetism in these systems are reported. Structurally, the overlayer relaxation is found to be less than 2% for both Ru/Ag(001) and Rh/Ag(001). FM ordering is confirmed to be the ground state for Rh/Ag(001) with a sizable magnetic moment of $0.96\mu_B$ /atom. However, an additional Ag overlayer diminishes the magnetic moment to $0.46\mu_B$ /atom, and more importantly, reduces drastically the energy of magnetization from 0.039 eV/atom to less than 0.005 eV/atom (which is essentially zero within the precision of the calculation). This destruction of the FM state appears to explain the lack of a FM signal in the SMOKE experiments.^{22,23} A considerable charge redistribution (accumulated in the interfacial region) is found which suggests a strong Rh-Ag interaction. Contrary to the result of Eriksson, Albers, and Boring,¹⁹ the FM state lies much lower in energy than the PM state for both Ru/Ag(001) and Ag/Ru/Ag(001)—which provides a more suitable system for experimental verification of 4d ferromagnetism than does Rh. In the following, the methodology and computational details are given in Sec. II, results and discussions (including the total-energy analysis, magnetic properties, overlayer-substrate interac-

tion, and single-particle spectra, etc.) are presented in Sec. III, and some conclusions are given in Sec. IV.

II. METHODOLOGY AND COMPUTATIONAL DETAILS

The Ag(001) substrate is simulated by an ideally constructed 5-layer slab with the lattice constant chosen from experiment ($a = 5.460$ a.u.). For the adsorption systems, adatoms are put pseudomorphically over the four-fold hollow sites on both sides of the substrate slab. For Rh/Ag(001) and Ru/Ag(001), the overlayer relaxation was determined by using total-energy minimization, while unrelaxed interatomic distances ($d_{\text{Rh-Ag}} = 5.272$ a.u., $d_{\text{Ru-Ag}} = 5.228$ a.u.) were employed for Ag/Rh/Ag(001) and Ag/Ru/Ag(001).

In the FLAPW approach, no shape approximations are made to the charge densities, potentials, and matrix elements. The core states are treated fully relativistically and the valence states are treated semirelativistically (i.e., without spin-orbit coupling).²⁴ The Hedin-Lundqvist and the von Barth-Hedin formulas for the exchange-correlation potentials are employed for the nonmagnetic and the spin-polarized calculations, respectively.²⁵ About 70 augmented plane waves per atom are used as a variational basis set (corresponding to an energy cutoff of 11 Ry). Within the muffin-tin (MT) spheres, lattice harmonics with angular-momentum l up to 8 are used to expand the charge density, potential, and wave functions. Integrations over k space are substituted by summations over 15 special k points in the $\frac{1}{8}$ irreducible two-dimensional (2D) Brillouin zone (BZ).²⁶ Convergence is assumed when the average root-mean-square distance between the input and output charge and spin densities is less than 2×10^{-4} e/(a.u.).³ Consequently, total-energy differences are reliable up to 1 mRy.

III. RESULTS AND DISCUSSIONS

A. Total-energy analysis

The calculated total energies versus the distance between adatom and the nearest Ag atoms are presented for Ru/Ag(001) and Rh/Ag(001) in Fig. 1. Clearly, the calculated data can be well fitted by a parabola (solid lines), which indicates the precision of the calculated total energies. For Ru/Ag(001), the equilibrium $d_{\text{Ru-Ag}}$ is 5.21 a.u. for both the PM and FM states, which decreases by only 0.3% from the ideal value, 5.228 a.u. (defined as the average of the interatomic distances in bulk Ag and Ru). For Rh/Ag(001), the equilibrium $d_{\text{Rh-Ag}}$ is 5.18 and 5.14 a.u. for the FM and the PM states, respectively—amounting to 1.7% and 2.5% downward relaxations compared to the ideal distance, 5.272 a.u. This suggests that the distances used by Eriksson, Albers, and Boring¹⁹ [5.46 a.u., for Rh/Ag(001)] and Zhu, Bylander, and Kleinman¹⁸ [5.36 a.u., for Rh/Au(001)] were too large. Unlike those cases with strong interfacial interaction [e.g., Fe/Ru(0001) (Ref. 27)], the effect of overlayer relaxation on the magnetization is found to be negligible here.

Clearly, the energy of the FM state is lower than the PM state for both systems—which indicates that the FM

ordering is truly the stable ground state for both Ru/Ag(001) and Rh/Ag(001). For Rh/Ag(001), we obtained a magnetization energy (defined as the difference between the total-energy minima of the FM and PM states) of 0.04 eV/adatom, which is about 2.5 times larger than the result of Eriksson, Albers, and Boring (0.016 eV).¹⁹ Furthermore, we found that FM ordering is also the stable ground state for Ru/Ag(001) (with an even larger magnetic energy of 0.076 eV/adatom). This result differs from the report of Eriksson, Albers, and Boring that the FM state can exist only as a metastable state. To clarify the interfacial effect with the Ag substrate and the

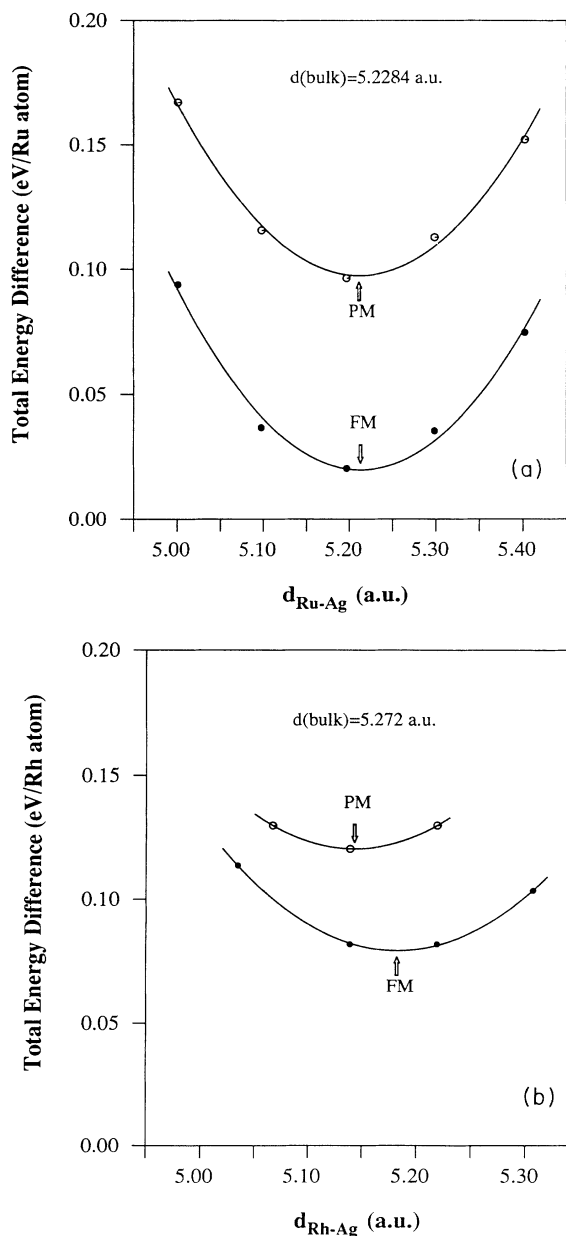


FIG. 1. Theoretical total energy of (a) Ru/Ag(001) and (b) Rh/Ag(001) vs Ru(Rh)-Ag distance. The open and solid circles represent the results for the PM and FM states, respectively. The solid lines are the fitting parabolas. Arrows show the corresponding minimum energy positions.

TABLE I. The energy of magnetization E (in eV/adatom), work function Φ (in eV), magnetic moment M (in μ_B) in the Rh and Ru muffin-tin spheres, and the ratio of the core contribution to the hyperfine field $H_{CF,c}$ to the magnetic moment M (in kG/μ_B) for Rh and Ru monolayers when free standing (ML), deposited on the Ag(001) substrate, and sandwiched by an additional Ag layer.

System	E	Φ	M	$H_{CF,c}/M$
Rh ML	0.073	5.77	1.45	-407
Rh/Ag(001)	0.040	5.52	0.96	-401
Ag/Rh/Ag(001)	< 0.005	4.87	0.49	-399
Ru ML	0.100	5.32	2.12	-407
Ru/Ag(001)	0.076	5.28	1.57	-408
Ag/Ru/Ag(001)	0.040	4.77	1.13	-396

effect of an additional Ag overlayer, the magnetic energies of Ru and Rh monolayers are listed in Table I for these metals (i) as free monolayers, (ii) when adsorbed on the Ag(001) substrate, and (iii) when sandwiched by the additional Ag overlayer. Obviously, for both Rh and Ru, the larger the number of interfaces, the smaller the magnetic energy. Thus, as was seen for the 3d systems,⁴ interfacial effects with Ag(001) are detrimental to the magnetic polarization of the Rh and Ru overlayers.

Note that the magnetic energy for Ag/Rh/Ag(001) is too small to identify meaningfully in the FLAPW total-energy calculations (< 0.5 mRy/cell). Therefore, the FM state is no longer the stable ground state—which appears to explain the lack of the FM signal in the SMOKE experiments of Mulhollan, Fink, and Erskine and Liu and Bader.^{22,23} By contrast, as shown in Table I, the magnetic energy for Ag/Ru/Ag(001) is still as large as 0.04 eV per Ru atom. Therefore, Ru appears to be a more suitable 4d element for experimental verification of 4d ferromagnetism, and thus we will center the following discussion on Ru/Ag(001).

B. Density of states

Physically, magnetism in the 4d metal monolayers results from the narrowed energy bands which leads to a large density of states at E_F [$N(E_F)$]. For example, the $N(E_F)$ of PM Ru and Rh monolayers are found to increase by 450% over their corresponding bulk values,²⁸ which results in a large Stoner factor (1.45 and 1.89 for Ru and Rh monolayers, respectively) and thus a Stoner instability.

The density of states (DOS) projected in each muffin-tin sphere for FM Ru/Ag(001) is plotted by solid lines in Fig. 2(a) (majority spin) and 2(b) (minority spin) and compared with the corresponding results (dotted lines) for the isolated FM Ru monolayer and (per spin) for the PM Ag(001) clean surface. For the isolated FM Ru monolayer, the average exchange splitting is about 1.5 eV, so the Fermi energy avoids lying just on the PM antibonding peak. Surprisingly, the majority-spin 4d band is still not fully occupied (i.e., it has a small number of holes), although that of its isoelectronic 3d counterpart, Fe, lies almost 2.5 below E_F . For the clean Ag(001) surface, the

DOS of the surface layer is obviously narrower than those for the interior Ag layers due to the loss of atomic coordination. From the DOS curves (solid lines) for Ru/Ag(001), a strong mutual influence between Ru and Ag can be seen. Clearly, the states of the interfacial Ag layer extend their tails into the Ru spheres for both majority- and minority-spin states, which pushes up the

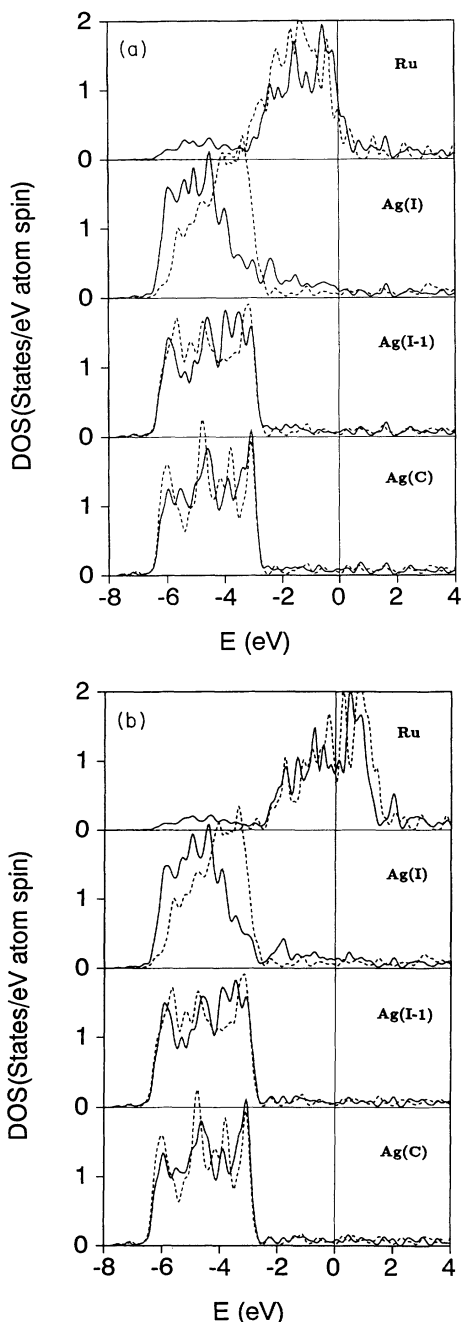


FIG. 2. The projected density of states of Ru/Ag(001) in each muffin-tin sphere for (a) majority spin and (b) minority spin. In the panels for Ru, the dotted lines represent the results for the FM Ru monolayer; in the panels for Ag, they are given per spin [i.e., equal to half of the corresponding results of the PM Ag(001) surface]. Energy scales are shifted with respect to E_F , taken in each case as the zero of energy.

majority-spin bands of Ru (thus creating more majority-spin 4d holes) to maintain charge neutrality, and hence to diminish the overlayer magnetism. In turn, the presence of the Ru adlayer lowers the potential in the interfacial region and thus states of the interfacial Ag layer drop down markedly. However, since there is no noticeable overlayer-substrate band overlap (except for the extension of the wave-function tails), the Ru and Ag layers interact mainly via electrostatic effects in the interfacial region rather than via covalent bonding. Furthermore, an efficient (i.e., short range) metallic screening is also obviously seen whereas no significant change is found on the DOS curves for the interior Ag layers.

To see the influence of the additional Ag layer on the magnetism, the DOS in the Ru muffin-tin sphere for Ag/Ru/Ag(001) (solid lines) is plotted in Fig. 3, where the accompanying curves (dashed lines) are for Ru/Ag(001). Obviously, the interfacial effect is almost doubled, i.e., the Ru muffin-tin spheres gets more tails from the Ag wave function while the majority-spin 4d bands of Ru are pushed further upwards—which, of course, reduces the magnetism in the Ru layer.

Since the 3d atoms are smaller in size and in addition the majority-spin bands lie well below the Fermi level, inert substrates [e.g., Ag(001)] affect the 3d overlayer magnetism mainly via a transfer of minority-spin electrons and an induced on-site *sp-d* rehybridization; both effects have been confirmed to be very weak for 3d noble-metal systems.^{4,29} By contrast, the 4d function extends into a larger spatial region and hence overlaps more with the wave functions of the substrate atoms. Although they do not hybridize significantly because of the large separation on the energy scale, the wave-function overlap certainly induces a stronger overlayer-substrate mutual influence via the Coulomb (i.e., orthogonality) repulsion.

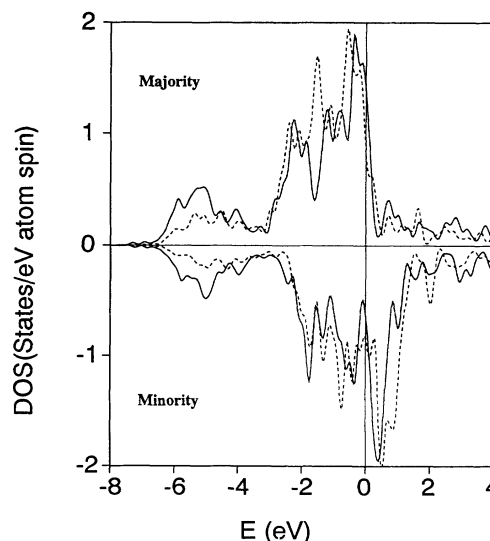


FIG. 3. The projected Ru density of states in Ag/Ru/Ag(001), denoted by solid lines, and in Ru/Ag(001), denoted by dotted lines.

C. Charge-density and overlayer-substrate interaction

Figure 4 plots the total charge density for the Ru ML, the Ag(001) clean surface, Ru/Ag(001), and Ag/Ru/Ag(001). The metallic screening effect is obvious in this figure since the contours just under the surface Ag atomic plane are very similar in all three cases. Furthermore, we find a charge accumulation in the interfacial region in panels 4(b) and 4(c), whereas the charge density between Ru-Ag becomes even larger than that between Ag-Ag.

A clearer insight into the overlayer-substrate interaction is given by the charge-density difference $\rho_{\text{Ru/Ag(001)}} - \rho_{\text{Ag(001)}} - \rho_{\text{Ru ML}}$ in Fig. 5(a), and $\rho_{\text{Ag/Ru/Ag(001)}} - \rho_{\text{Ru/Ag(001)}} - \rho_{\text{Ag ML}}$ in Fig. 5(b). In panel 5(a), a strong mutual Ru-Ag influence is clearly visible. The Ru atom gets increased occupation for the d_{z^2} state but loses d_{xz} -like electrons. On the other hand, interfacial Ag atoms lose electrons in the region around their nuclei but gain s, p electrons in the hollow site and in the interfacial region. As discussed above, this happens because of the overlayer-induced lowering of the potential rather than covalent bonding. Thus, the effect of the Ag(001) substrate cannot be neglected. Note that the perturbation in the interfacial region decays quickly and shows an oscillation when approaching into the interior of the substrate—which indicates the effect of substrate metallic screening. In Fig. 5(b), the same effect appears in the other Ru-Ag(A) interface. Moreover, the charge density is practically unmodified in the first [Ru-Ag(I)] interfacial region with additional Ag coverage. Therefore, the effects of the two interfaces actually can be considered separately and so to be double that of one interface.

The calculated work functions, which characterize the metal surface barriers, are also given in Table I. The value for the clean Ag(001) surface, 4.60 eV is a little smaller compared to the earlier result given by Erschbaumer *et al.*³⁰ of 4.74 eV obtained from an 11-layer slab, but is larger than experimental values (4.22–4.43 eV).³¹

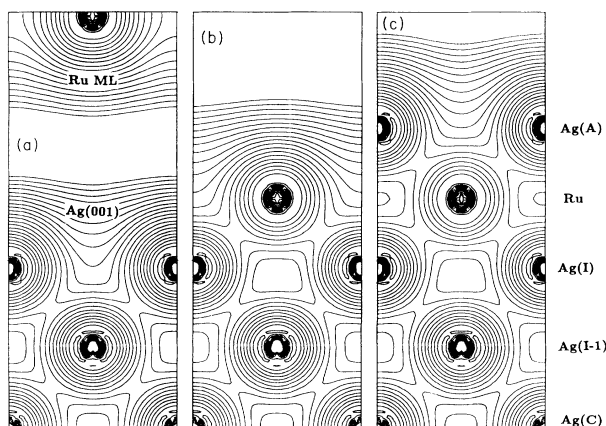


FIG. 4. The total charge density of (a) the free Ru ML and Ag(001) clean surface, (b) Ru/Ag(001), and (c) Ag/Ru/Ag(001) on a vertical (110) plane. Contours start from 5×10^{-4} e/a.u.³ and increase successively by a factor of $\sqrt{2}$.

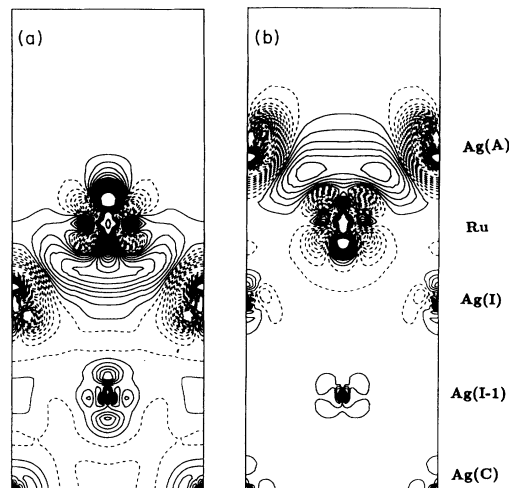


FIG. 5. Charge-density difference (a) between Ru/Ag(001) and the direct superposition from the free Ru ML and the clean Ag(001) surface and (b) between Ag/Ru/Ag(001) and the direct superposition of the free Ag ML and Ru/Ag(001). Contours shown on the same vertical plane as in Fig. 4 start from $\pm 5 \times 10^{-4}$ e/a.u.³ and change successively in steps of $\pm 1 \times 10^{-3}$ e/a.u.³. Solid and dashed lines represent positive and negative differences, respectively.

[The discrepancy may be attributed to either (i) the fact that the experimental values are usually depressed by surface roughness, which is a particular problem with silver, or (ii) that a very careful theoretical treatment, e.g., using a large enough number of k points and plane waves, may be essential to get a correct work function for Ag(001).³²] The work function for the FM Rh (Ru) monolayer is 5.77 eV (5.32 eV), which is also close to the pseudopotential results, 5.73 eV, for Rh on the Au(001) substrate.¹⁸ For Rh/Ag(001) and Ru/Ag(001), the work functions are close to the values for the isolated Rh and Ru monolayers despite the considerable charge redistribution—indicative of the strong screening effect in the overlayers. For the same reason, the additional Ag coverage lowers the work functions drastically toward the value of the Ag(001) substrate. Experimental measurements are eagerly awaited as a check of these predicted results.

D. Magnetic polarization and hyperfine field

Figure 6 presents spin-density contours on the vertical (110) plane for (a) the isolated Ru monolayer, (b) Ru/Ag(001), and (c) Ag/Ru/Ag(001). Generally, the spin density of this $4d$ metal is similar to that of the $3d$ series, i.e., with a positive spin density in a large region around the nucleus and with a small packet of negative spin density in the interstitial region. By comparing panels 6(b) and 6(c) to panel 6(a), the area of positive spin density is markedly depressed in the interfacial region, which indicates the detrimental effect of the Ag(001) substrate on the magnetization in the Ru monolayer. Moreover, due to the efficient metallic screening by the noble metal, the magnetic influence of the Ru monolayer is limited only to within the interfacial layer into the Ag(001) substrate.

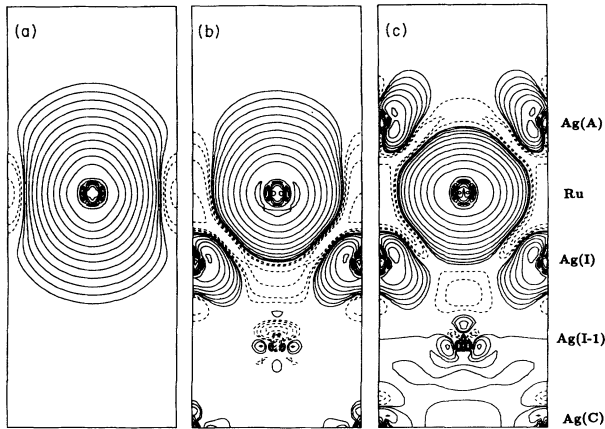


FIG. 6. The theoretical spin density for (a) Ru ML, (b) Ru/Ag(001), and (c) Ag/Ru/Ag(001). Contours shown on the same vertical as in Fig. 4 start from $\pm 1 \times 10^{-4}$ e/a.u.³ and increase successively by a factor of ± 2 . The solid and dashed lines indicate positive and negative spin density, respectively.

The integrated spin density, i.e., the magnetic moments in the Ru (and Rh) muffin-tin spheres ($r_{\text{MT}} = 2.50$ a.u.), are also listed in Table I. For the Rh monolayer, a sizable magnetic moment of $1.46\mu_B$ is found, which is about 35% smaller, however, than that for its isoelectronic 3d (Co) monolayer, $2.2\mu_B$.¹³ This magnetic moment decreases drastically by as much as 35% to $0.96\mu_B$ after being deposited on the Ag(001) substrate, and, furthermore, drops to $0.49\mu_B$ after being sandwiched by the additional Ag layer. By comparison, the magnetic moment of the Co monolayer only decreases by $0.17\mu_B$ (7.7%) on Ag(001) from the value in the free monolayer case. Thus, 4d metals respond to the change of the environment much more sensitively than do 3d metals, because of the larger spatial extent of their valence wave function. Upon going to the left in the Periodic Table to Ru, as also revealed for the 3d series,¹³ the 4d magnetic moments increase by $\sim 0.65\mu_B$ (instead of $\sim 1.0\mu_B$ for Fe

and Co) due to the existence of 4d majority-spin holes in almost all the environments. Therefore, from the point of view of both larger magnetic energy and stronger magnetism, Ru/Ag(001) offers a better opportunity for experimental verification studies than does Rh/Ag(001).

The Fermi contact hyperfine field H_{CF} describes the well-known coupling between the electronic spin and the nuclear magnetic moment, and is proportional to the electronic spin density at the nucleus. It is usually divided into contributions from core and valence electrons; as established for the 3d magnetic systems, the core contribution (negative in sign) is proportional to the local moment.^{4,29,33} For 4d systems, as listed in Table I, the proportionality still remains, while the ratio of the core contribution to the magnetic moment (~ 400 kG/ μ_B) is much larger than that for the 3d series (~ 140 kG/ μ_B). An orbital decomposition indicates that the 4s,p shells also give a negative contribution as do the inner 1s and 2s,p shells, which differs from the 3d systems and Gd that outer shells give a positive contribution.^{4,34} However, the valence contribution $H_{\text{CF},v}$, and thus H_{CF} itself, depend on the choice of k points very sensitively. For example, the total hyperfine field for Rh/Ag(001) decreases monotonically from 161 kG for 15 k points (in $\frac{1}{8}$ irreducible 2D BZ) to 70 kG for 21 k points and further to 45 kG for 28 k points, and so too for Ru/Ag(001). From this trend, we can infer that the net H_{CF} should be very small for 4d magnetic systems, and thus it should be hard to detect the effect of 4d magnetism in those experiments which rely on the hyperfine field interaction, e.g., NMR, etc.

ACKNOWLEDGMENTS

Work at Northwestern University was supported by the National Science Foundation [(Grant No. DMR88-16126) and by a grant of computer time at the Pittsburgh Supercomputing Center through its Division of Advanced Scientific Computing]. Work at Argonne National Laboratory was supported by the Department of Energy.

¹L. M. Falicov, D. T. Pierce, S. D. Bader, R. Gronsky, K. B. Hathaway, H. J. Hopster, D. N. Lambeth, S. P. Parkin, G. Prinz, M. Salamon, I. K. Schuller, and R. H. Victora, *J. Mater. Res.* **5**, 1299 (1990).

²S. D. Bader, *Proc. IEEE* **78**, 909 (1990).

³C. L. Fu, A. J. Freeman, and T. Oguchi, *Phys. Rev. Lett.* **54**, 2700 (1985).

⁴A. J. Freeman and R. Wu, *J. Magn. Magn. Mater.* **100**, 497 (1991).

⁵M. B. Brodsky and A. J. Freeman, *Phys. Rev. Lett.* **45**, 133 (1980).

⁶M. B. Brodsky, *J. Phys. (Paris) Colloq.* **45**, C5-349 (1984).

⁷T. Jarlborg and A. J. Freeman, *Phys. Rev. B* **23**, 3577 (1981); *Physica B* **107**, 69 (1981).

⁸S. C. Hong, C. L. Fu, and A. J. Freeman, *J. Appl. Phys.* **63**, 3655 (1988).

⁹V. L. Moruzzi and P. M. Marcus, *Phys. Rev. B* **39**, 471 (1989), **42**, 10322 (1990).

¹⁰H. Chen, N. E. Brener, and J. Callaway, *Phys. Rev. B* **40**, 1443 (1989).

¹¹M. J. Zhu, D. M. Bylander, and L. Kleinman, *Phys. Rev. B* **42**, 2874 (1990).

¹²C. Li, *Bull. Am. Phys. Soc.* **36**, 677 (1991).

¹³S. Blügel, B. Drittler, R. Zeller, and P. H. Dederichs, *Appl. Phys. A* **49**, 547 (1989).

¹⁴C. L. Fu and A. J. Freeman, *J. Phys. (Paris) Colloq.* **49**, C3-1625 (1988).

¹⁵S. C. Hong, A. J. Freeman, and C. L. Fu, *Phys. Rev. B* **39**, 5719 (1989).

¹⁶R. L. Fink, C. A. Ballentine, J. L. Erskine, and J. A. Araya-Pochet, *Phys. Rev. B* **41**, 10175 (1990).

¹⁷R. Wu, C. Li and A. J. Freeman, *J. Magn. Magn. Mater.* **99**, 71 (1991).

¹⁸M. J. Zhu, D. M. Bylander, and L. Kleinman, *Phys. Rev. B* **43**, 4007 (1991).

¹⁹O. Eriksson, R. C. Albers, and A. M. Boring, *Phys. Rev. Lett.*

- 66, 1350 (1991).
- ²⁰K. Schwarz and P. Mohn, *J. Phys. F* **14**, L129 (1984).
- ²¹E. R. Moog and S. D. Bader, *Superlatt. Microstruct.* **1**, 543 (1985); C. Liu, E. R. Moog, and S. D. Bader, *Phys. Rev. Lett.* **60**, 2422 (1988); *J. Appl. Phys.* **64**, 5325 (1988).
- ²²G. A. Mulhollan, R. L. Fink, and J. L. Erskine, *Phys. Rev. B* **44**, 2393 (1991).
- ²³C. Liu and S. D. Bader, *Phys. Rev. B* **44**, 12 062 (1991).
- ²⁴D. D. Koelling and B. N. Harmon, *J. Phys. C* **10**, 3107 (1977).
- ²⁵L. Hedin and B. I. Lundqvist, *J. Phys. C* **4**, 2064 (1971); U. von Barth and L. Hedin, *ibid.* **5**, 1629 (1972).
- ²⁶S. L. Cunningham, *Phys. Rev. B* **10**, 4988 (1974).
- ²⁷R. Wu and A. J. Freeman, *Phys. Rev. B* **44**, 4449 (1991).
- ²⁸J. F. Janak, *Phys. Rev. B* **16**, 255 (1977).
- ²⁹A. J. Freeman, C. L. Fu, S. Ohnishi, and M. Weinert, in *Polarized Electrons in Surface Physics*, edited by R. Feder (World Scientific, Singapore, 1985).
- ³⁰H. Erschbaumer, A. J. Freeman, C. L. Fu, and R. Podloucky, *Surf. Sci.* **243**, 317 (1991).
- ³¹M. Chelvayohan and C. H. B. Mee, *J. Phys. C* **xx**, 2305 (1982); K. Giesen, F. Hage, F. J. Himpsel, H. J. Riess, and W. Steinmann, *Phys. Rev. B* **35**, 971 (1987); R. W. Schoenlein, J. G. Fujimoto, G. L. Eesley, and T. W. Capehart, *Phys. Rev. Lett.* **61**, 2596 (1988).
- ³²Indeed, different methods yield results ranging from 4.2 to 4.95 eV, cf. J. R. Smith, F. J. Arlinghaus, and J. G. Gay, *Phys. Rev. B* **22**, 4757 (1980); D. R. Hamann, L. F. Mattheiss, and H. S. Greenside, **24**, 6151 (1981); G. C. Aers and J. E. Inglesfield, *Surf. Sci.* **217**, 367 (1987).
- ³³A. J. Freeman and R. E. Watson, in *Magnetism*, edited by G. T. Rado and H. Suhl (Academic, New York, 1965), Vol. II A, p. 167.
- ³⁴Ruqian Wu, Chun Li, A. J. Freeman, and C. L. Fu, *Phys. Rev. B* **44**, 9400 (1991).